Original Article

SMARCA4/BRG1-deficient non-small cell lung cancer: clinical, imaging, pathological features, and follow-up results of 23 patients

Xieraili Wumener[1,2#], Xiaoxing Ye[3#], Yarong Zhang[2], Tuya E[4], Jiuhui Zhao[2], Ying Liang[2], Jun Zhao[5]

[1]Department of Graduate School, Dalian Medical University, Dalian, China; [2]Department of Nuclear Medicine, National Cancer Center/National Clinical Research Center for Cancer/Cancer Hospital & Shenzhen Hospital, Chinese Academy of Medical Sciences and Peking Union Medical College/Shenzhen Clinical Research Center for Cancer, Shenzhen, China; [3]Department of pathology, National Cancer Center/National Clinical Research Center for Cancer/Cancer Hospital & Shenzhen Hospital, Chinese Academy of Medical Sciences and Peking Union Medical College/Shenzhen Clinical Research Center for Cancer, Shenzhen, China; [4]Department of Radiology, National Cancer Center/National Clinical Research Center for Cancer/Cancer Hospital & Shenzhen Hospital, Chinese Academy of Medical Sciences and Peking Union Medical College/Shenzhen Clinical Research Center for Cancer, Shenzhen, China; [5]Department of Nuclear Medicine, Shanghai East Hospital Tongji University, Shanghai, China

Contributions: (I) Conception and design: X Wumener; (II) Administrative support: Jun Zhao, Y Liang; (III) Provision of study materials or patients: X Ye; (IV) Collection and assembly of data: T E, Jiuhui Zhao; (V) Data analysis and interpretation: Y Zhang; (VI) Manuscript writing: All authors; (VII) Final approval of manuscript: All authors.

[#]These authors contributed equally to this work.

Correspondence to: Jun Zhao, MD, PhD. Department of Nuclear Medicine, Shanghai East Hospital Tongji University, No. 150 Jimo Road, Pudong New Area, Shanghai 200120, China. Email: petcenter@126.com; Ying Liang, MD, PhD. Department of Nuclear Medicine, National Cancer Center/National Clinical Research Center for Cancer/Cancer Hospital & Shenzhen Hospital, Chinese Academy of Medical Sciences and Peking Union Medical College/Shenzhen Clinical Research Center for Cancer, No. 113, Baohe Road, Longgang District, Shenzhen 518117, China. Email: liangying_473@163.com.

Background: *SMARCA4*/BRG1-deficient non-small cell lung cancer (S/B-d NSCLC) is a rare subtype of non-small cell lung cancer (NSCLC). The aim of this study was to investigate the clinical, imaging, serum tumor marker, and pathological features of S/B-d NSCLC, particularly computed tomography (CT) and ^{18}F-fluorodeoxyglucose (FDG) positron emission tomography-computed tomography (PET/CT) scan features.

Methods: Our analysis included 23 patients with pathologically confirmed S/B-d NSCLC from January 2021 to December 2023. A retrospective analysis of clinical, serum tumor markers, imaging [including CT, FDG PET/CT, magnetic resonance imaging (MRI)], pathological features, treatment protocols, and follow-up results was performed. Independent samples *t*-tests were used to assess statistical differences in short diameters and maximum standardized uptake value (SUV_{max}) between groups.

Results: S/B-d NSCLC occurs predominantly in male patients with a history of smoking and a mean age of 62.78 years (39–77 years). S/B-d NSCLC was found incidentally during physical examination in 56.52% of patients. The CT scan features were as follows: predominantly tumors (72.73%), peripheral in the lungs (77.27%), round or roundish morphology (81.28%), pleural or vascular invasion (95.46%), and moderately to severely enhanced (59.09%). The FDG PET/CT showed FDG-avid with mean SUV_{max} of 14.78±9.57. Lung cancer-related serum tumor markers had high positivity rates for carcinoembryonic antigen (CEA) (66.67%), recombinant cytokeratin fragment antigen 21-1 (CYFRA21-1) (61.91%), and carbohydrate antigen 125 (CA125) (57.14%). Pathological features are often characterized by grading (poor differentiation, 100%), tumor spread through the air space (STAS, 85.71%), and vascular invasion (85.71%). Immunohistochemistry showed that *SMARCA4* (BRG1) was absent, and P40, P63, ALK-Ventana ALK (D5F3), and p-TRK were often negative. Genetic tests showed that the positivity rate of TP53 (76.92%) and KEAP1 (53.85%) was high. Despite diverse treatment options being available, high rates of progression during treatment and poor

prognosis were observed. Among CT features (N=22), the short diameter of CT-diagnosed metastatic lymph nodes (LNs) was larger than that of non-metastatic LNs, and the difference was statistically significant (P=0.02). Among the FDG PET/CT features (N=12), SUV_{max} was larger in tumor group than lesion group, SUV_{max} was larger in M1 group than M0 group, and the difference was statistically significant in both groups (P=0.001 and P=0.04).

Conclusions: S/B-d NSCLC has distinct features in epidemiology, serum tumor markers, imaging, and pathology. In particular, FDG-avid is evident in the FDG PET/CT scan. The size of the lesion and the degree of FDG avidity provide information about the degree of malignancy and the high probability of distant metastasis in S/B-d NSCLC. FDG PET/CT is recommended when S/B-d NSCLC is suspected based on CT features, especially for large lesions. The FDG PET/CT scan can help with accurate staging and individual treatment planning.

Keywords: *SMARCA4*/BRG1-deficient non-small cell lung cancer (S/B-d NSCLC); computed tomography (CT); positron emission tomography-computed tomography (PET/CT); lung cancer

Submitted Jul 03, 2024. Accepted for publication Dec 19, 2024. Published online Jan 22, 2025.
doi: 10.21037/tlcr-24-567
View this article at: https://dx.doi.org/10.21037/tlcr-24-567

Introduction

SMARCA4/BRG1-deficient non-small cell lung cancer (S/B-d NSCLC) is a rare subtype of non-small cell lung cancer (NSCLC) (1). S/B-d NSCLC was first reported by Wong *et al.* in 2000 and has only emerged as a distinct subgroup of NSCLC in recent years (2,3).

The *SMARCA4* gene is located on chromosome 19P13 and encodes BRG1 (4). BRG1 is one of the most abundant aberrant adenosine triphosphate (ATP)-dependent catalytic subunits of SWI tch/sucrose non-fermentable (SWI/SNF) chromatin remodeling complexes, which are involved in the activation or repression of transcriptional processes in various cancers (5,6). Previous studies have reported that *SMARCA4* mutations occur in approximately 5–16% of primary lung cancers and 10% of NSCLC cases (7,8).

S/B-d NSCLC is an poorly differentiated aggressive lung cancer that is strongly associated with smoking and commonly occurs in men aged 40–50 years (3,9). Deletion of *SMARCA4*/BRG1 not only increases tumor invasiveness and metastasis incidence, but is also associated with the development of drug-resistant tumors, recurrence, and a less favorable prognosis (7,10-12). S/B-d NSCLC occurs predominantly in pleural and vascular segments (3,9). It is very aggressive, rapidly progressive, and has a poor prognosis (7,11-13), regardless of tumor, node, metastasis (TNM) stage (3,9,14,15). Previous studies have reported that approximately 83% of S/B-d NSCLCs are already stage IV at the time of discovery and have a progression-free survival of only 30 days (11,16).

In recent years, studies on the diagnosis, treatment, and prognosis of S/B-d NSCLC have attracted the attention of many physicians and researchers. Due to the rarity of the disease, more previous studies were conducted on the diagnostic aspects of the pathology, with fewer studies

Highlight box

Key findings
- *SMARCA4*/BRG1-deficient non-small cell lung cancer (S/B-d NSCLC) has distinct features in epidemiology, serum tumor markers, imaging, and pathology.

What is known and what is new?
- S/B-d NSCLC is a rare subtype of NSCLC.
- S/B-d NSCLC computed tomography (CT) scan features are short diameter >3.0 cm, in the lung area of peripheral, round or roundish morphology, pleural or vascular invasion, and moderate-to-severe on enhanced scans reinforced. The 18F-fluorodeoxyglucose (FDG) positron emission tomography-computed tomography (PET/CT) showed that FDG-avidity with mean maximum standardized uptake value of 14.78±9.57, size of the lesion, and the degree of FDG avidity provide information about the degree of malignancy and the high probability of distant metastasis in S/B-d NSCLC.

What is the implication, and what should change now?
- FDG PET/CT is recommended when S/B-d NSCLC is suspected based on CT features, especially for large lesions. The FDG PET/CT scan can help with accurate staging and individual treatment planning.

having investigated the imaging features, particularly the ^{18}F-fluorodeoxyglucose (FDG) positron emission tomography-computed tomography (PET/CT) features (1,12,15-17). Previous imaging studies of S/B-d NSCLC have predominantly been case reports (18-20). Currently it is 2023, and we have endeavored to present case reports on the use of dynamic and static FDG PET/CT imaging in S/B-d NSCLC and response to treatment (20). It is crucial to determine the imaging features of this rare tumor. Therefore, we summarized the clinical, imaging, and pathological features and follow-up results of 23 patients with S/B-d NSCLC to further elucidate the clinical and pathological features and try to identify specific imaging features that could contribute to the diagnosis of the disease. We present this article in accordance with the STROBE reporting checklist (available at https://tlcr.amegroups.com/article/view/10.21037/tlcr-24-567/rc).

Methods

Patients

Patients were identified through the pathology database, medical record system, and picture archiving and communication system (PACS) of Cancer Hospital & Shenzhen Hospital, Chinese Academy of Medical Sciences and Peking Union Medical College. We included 23 patients with a pathologically confirmed diagnosis of S/B-d NSCLC with complete clinical, imaging, and pathological data from January 2021 to December 2023.

The study was conducted in accordance with the Declaration of Helsinki (as revised in 2013). The study was approved by the Ethics Committee of National Cancer Center/National Clinical Research Center for Cancer/Cancer Hospital & Shenzhen Hospital, Chinese Academy of Medical Sciences and Peking Union Medical College/Shenzhen Clinical Research Center for Cancer (No. KYKT2024-19-1). All patients consented to the collection of medical information at their first visit. Inform consent is not required due to the retrospective nature of this study.

Clinical features

Patient clinical information was collected from the medical record system, including age, gender, place of origin, clinical presentation (first visit), American Joint Committee on Cancer (AJCC) stage (21), smoking history (a heavy smoker was defined by ≥20 pack-years), family history of the tumor, and tumor markers associated with lung cancer. Lung cancer-related serum tumor markers including carcinoembryonic antigen (CEA, 0–5.0 ng/mL), pro-gastrin-releasing peptide (Pro GRP, <69.2 pg/mL), recombinant cytokeratin fragment antigen 21-1 (CYFRA21-1, <3.3 ng/mL), carbohydrate antigen 125 (CA125, <35.0 U/mL), neuron-specific enolase (NSE, <16.3 ng/mL), and squamous cell carcinoma antigen (SCC, <2.7 ng/mL).

CT and magnetic resonance imaging (MRI) scans

All chest CT scans were performed using either 64-row or 256-row multidetector scanners (Optima or Revolutions, GE Medical Systems, Milwaukee, WI, USA). All scans were performed in the supine position. The examinations were initially carried out with a non-contrast series and then with a two-phase contrast medium series. Venous phase scanning began 50 seconds after the trigger attenuation threshold [120 Hounsfield unit (HU)] reached the level of the thoracic aorta. The intravenous contrast agent (Ultravist 300 or 370, Bayer Schering Pharma, Berlin, Germany; Ioversol 350, Jiangsu Hengrui Pharmaceuticals Co., Ltd., Lianyungang, China) was administered at a rate of 2.5–3.0 mL/s (1.1–1.3 mL/kg injected body weight). The following imaging parameters were applied: slice thickness of 5 mm, 120 kVp, 100–500 Smart mAs, noise index of 10.5 or 15, pitch of 0.516, 0.992, or 1.375.

The chest MRI scan was performed using a 3.0 T whole-body MRI scanner (Ingenia, Philips Healthcare, Best, The Netherlands) with a 16-channel body receiver coil. The scanning area extended from the level of the apex of the lung to the adrenal glands. The MRI sequences included breath-hold T2-weighted turbo-spin-echo imaging in the coronal planes, respiratory-triggering axial fat-suppressed T2-weighted turbo-spin-echo images, and respiratory-triggering axial diffusion-weighted single images with a b value of 500 s/mm^2 and breath-hold T1-weighted Dixon in the axial plane without contrast. Then, the breath-hold T1-weighted Dixon was acquired in an axial plane after intravenous injection of gadoteric acid meglumine salt injection (0.2 mL/kg, Jiangsu Hengrui Pharmaceuticals Co., Ltd., Lianyungang, China) in the arterial and venous phases followed by delayed phases in the coronal and sagittal planes.

The CT/MRI features were evaluated as follows: (I) lobe involved; (II) tumor site (peripheral or central: "central" meant that the tumor is located in the middle two-thirds of the lung and is closed to the mediastinum, main bronchi,

or central pulmonary vessels); (III) tumor short diameters; (IV) tumor size (lesion or tumor: "tumor" defined as short diameter pf lesion >3.0 cm); (V) morphology of the lesion (round or roundish or irregularly shaped); (VI) internal characteristics of the tumor, including the presence of necrosis, pleural and vascular involvement; (VII) pulmonary emphysema or pulmonary bulla; (VIII) pleural effusion; (IX) tumor density of CT scan (HU) or signal characteristics of MRI sequences; (X) degree of enhancement on enhanced scans (mild enhancement: increase in gain by 10–30 HU; moderate enhancement: increase in gain by 30–50 HU; strong enhancement: increase in gain by >50 HU); (XI) N-stage mediastinal or hilar lymph nodes (LNs) with a short-axis diameter of more than 1.0 cm were defined as positive LNs. N stage was based on the 8th edition of the TNM classification of lung cancer (22). The CT/MRI images were jointly diagnosed by two radiologists who had been working in diagnostics for 5 and 10 years, respectively. If there was a disagreement between the two physicians' diagnoses, a decision was made through general discussion.

FDG PET/CT scans

All patients fasted for at least 6 hours before scans were performed using the FDG PET/CT scanner (Discovery MI, GE Healthcare, Milwaukee, Wisconsin, USA). Blood glucose was maintained below 8.0 mmol/L. The FDG PET/CT scans were performed 60 minutes after injection of FDG (264.8±37 MBq) from an indwelling intravenous needle. Patients underwent a whole-body CT scan from the head to mid-femur in the supine, position with elevated arms. An additional whole body PET scan was performed. The CT parameters were tube voltage of 120 kV, tube current setting of 10–220 mA, pitch of 1.375:1, and noise index of 20. For the PET scan, the attenuation corrections were performed using CT data, and the reconstructions were performed using the block sequential regularized expectation maximization reconstruction algorithm (BSREM) with 25 iterations and 2 subsets.

Hematoxylin-eosin (HE), immunohistochemical (IHC) staining, and next-generation sequencing (NGS)

Lesion tissues were processed through formalin-fixed, paraffin-embedded tissue. HE and IHC staining were performed on whole slides containing 4 μm-thick tissue. Appropriate controls were used for each of the IHC staining sections. *SMARCA4* (anti-BRG1 antibody, clone E8V5B, ZSJQ-Bio, Beijing, China) was used to stain each tissue. Pan-CK (clone AE1/AE3, Gene Tech, Shanghai, China), TTF-1 (clone SP141, Roche, Basel, Switzerland), Napsin A (clone MRQ-60, Roche), CK7 (clone SP52, Roche), p40 (clone BC28, Roche), p63 (clone 4A4, Roche), CD56 (clone UMAB83, ZSGB-BIO), synaptophysin (clone SP11, Roche), chromogranin A (clone LK2H10, Roche), ALK (clone D5F3, Roche), Pan-TRK (clone EPR17341, Roche), Ki67 (clone 30-9, Roche), and programmed death ligand 1 (PD-L1) (clone 22C3, DAKO, Glostrup, Denmark) were performed on the available tumor tissue samples. The results of IHC staining were determined by the pathologist.

In 13 cases, abundant and well-preserved tumor tissue was available for NGS. DNA was extracted from paraffin-embedded tissue blocks using Concert RC1102 kits (BioVision, Milpitas, CA, USA). An enriched library containing all exons of 520 cancer-related gene panels was constructed using custom-made probes from Burning Rock Biotechnology (Guangzhou, China).

Statistical analysis

Presentation of continuous variables included mean and range, whereas categorical variables were expressed as counts and percentages (%). Independent samples *t*-tests were used to assess statistical differences in short diameters and maximum standardized uptake value (SUV_{max}) between groups. A P value of less than 0.05 was considered statistically significant. All statistical analyzes were performed in the statistical software R (version 4.1.1, R Foundation for Statistical Computing, Vienna, Austria).

Results

Clinical features

Table 1 summarizes the clinical features of 23 patients with S/B-d NSCLC. Of the 23 patients with S/B-d NSCLC, 22 (95.65%) were male and 1 (4.35%) was female. The mean age was 62.78±10.32 (range, 39–77) years. All 22 male patients had a history of smoking, including 20 heavy smokers. A total of 13 patients (56.52%) were asymptomatic at the time of initial diagnosis and were discovered incidentally during physical examination. Among the symptomatic patients, 5 (21.74%) had lung-related symptoms, including cough, sputum, hemoptysis, chest tightness, and shortness of breath, and 5 (21.74%) were seen

Table 1 Summary of clinical features of 23 S/B-d NSCLC patients

Characteristic	Values
Age (years)	62.78±10.32 [39–77]
Sex	
Male	22 (95.65)
Female	1 (4.35)
Smoking history (smoking cycle, years)	22 (95.65) [10–50]
Family history of tumors	2 (8.70)
Clinical manifestation	
Physical exam findings	13 (56.52)
Lung-related symptoms[†]	5 (21.74)
Symptoms caused by metastasis[‡]	5 (21.74)
T-staging	
T1	7 (30.44)
T2	5 (21.74)
T3	5 (21.74)
T4	6 (26.09)
N-staging	
N0	4 (17.39)
N1	4 (17.39)
N2	4 (17.39)
N3	11 (47.83)
M-staging	
M0	11 (47.83)
M1	12 (52.17)
AJCC-staging	
I	4 (17.39)
II	0
III	7 (30.44)
IV	12 (52.17)
Inspection methods	
CT	22 (95.65)
MRI	1 (4.35)
FDG PET/CT	12 (52.17)

Data are presented as mean ± SD [range] or n (%). [†], lung-related symptoms include: cough, sputum, hemoptysis, chest tightness, shortness of breath; [‡], symptoms caused by metastasis include: swollen lymph nodes on palpation, bone pain. S/B-d NSCLC, *SMARCA4*/BRG1-deficient non-small cell lung cancer; AJCC, American Joint Committee on Cancer; CT, computed tomography; MRI, magnetic resonance imaging; FDG PET/CT, ^{18}F-fluorodeoxyglucose positron emission tomography-computed tomography; SD, standard deviation.

for symptoms related to metastasis, including swollen LNs on palpation and bone pain. The AJCC stages of the 23 patients were as follows: stage I (N=4), stage II (N=0), stage III (N=7), and stage IV (N=12). Only 4 (17.39%) patients were in early stage (stage I and stage II) and 19 (82.61%) patients were in advanced stage (stage III and stage IV).

Of the 23 patients, 22 (95.65%) underwent CT scans to support diagnosis, of which 12 (52.17%) patients underwent further refinement of FDG PET/CT scan to support diagnosis and staging; 1 (4.35%) patient underwent chest MRI.

Serum tumor marker features

Of 23 S/B-d NSCLC patients, 21 underwent lung cancer-related tumor marker testing before treatment. *Table 2* shows a summary of serum tumor marker testing in these 21 patients. Among them, the positive rates of CEA, CYFRA21-1, and CA125 were high at 66.7%, 61.91%, and 57.14%, respectively.

CT features

Table 3 shows a summary of the chest CT features of the 22 S/B-d NSCLC patients. The mean short diameter of the 22 S/B-d NSCLC patients was 3.42±1.81 cm and 72.73% of the patients had a short diameter >3.0 cm. Some 77.27% of tumors were located in the periphery of the lung, most commonly in the right upper lobe (RUL) (31.82%) and left upper lobe (LUL) (36.36%). The main features of the CT scan included: round or roundish in 18 (81.82%) patients, pleural and vascular involvement in 21 (95.46%) patients, emphysema or pulmonary alveoli in 20 (90.91%) patients, and mild to moderate enhancement in 12 (54.55%) patients after enhancement scan. Chest CT scan was deemed to have positive LNs in 19 (86.36%) patients, with CT diagnosis was considered probable high stage N3 in 11 (50%) patients.

MRI features

A chest MRI scan was performed for 1 patient. The MRI features showed a tumor in the left lower lobe (LLL) with a size of 4.1 cm × 3.0 cm, with low signal in the T1-weight imaging (T1WI) sequence, an inhomogeneous high signal in the T2-weight imaging (T2WI) sequence, an inhomogeneous significant enhancement in the enhancement scan, and a necrotic area in the center of the lesion. In addition, the adjacent pleura was unevenly

Table 2 Summary of lung cancer-related tumor marker testing results in 21 S/B-d NSCLC patients

Characteristic	Range	Positive (N)	Negative (N)	% (positive/total)
CEA	1.15–22,443 ng/mL	14	7	66.67
Pro GRP	6.02–88.08 pg/mL	5	16	23.81
CYFRA21-1	1.63–91.17 ng/mL	13	8	61.91
CA125	4.1–1,709 U/mL	12	9	57.14
NSE	6.44–142.80 ng/mL	8	13	38.10
SCC	0.53–5.71 ng/mL	2	19	9.52

S/B-d NSCLC, *SMARCA4*/BRG1-deficient non-small cell lung cancer; CEA, carcinoembryonic antigen; Pro GRP, pro-gastrin-releasing peptide; CYFRA21-1, recombinant cytokeratin fragment antigen 21-1; CA125, carbohydrate antigen 125; NSE, neuron-specific enolase; SCC, squamous cell carcinoma antigen.

Table 3 Summary of CT features in 22 *SMARCA4*/BRG1-d NSCLC patients

Characteristic	Values
Tumor size (cm)	3.42±1.81
Tumor lobe involved	
RUL	7 (31.82)
RML	1 (4.55)
RLL	3 (13.64)
LUL	8 (36.36)
LLL	3 (13.64)
Tumor site in lobe	
Peripheral	17 (77.27)
Central	5 (22.73)
Tumor pattern	
Lesion	6 (27.27)
Tumor	16 (72.73)
Tumor morphology	
Round or roundish	18 (81.82)
Irregularly shaped	4 (18.18)
Internal characteristics	
Necrosis	5 (22.73)
Pleural and vascular involvement	21 (95.46)
Pulmonary emphysema or pulmonary bulla	20 (90.91)
Pleural effusion	4 (18.18)
Degree of enhancement	
Mild enhancement	9 (40.91)
Moderate enhancement	3 (13.64)
Strong enhancement	10 (45.46)
N-staging	
N (–)	3 (13.64)
N (+)	19 (86.36)
N0–2	11 (50.00)
N3	11 (50.00)

Data are presented as mean ± SD or n (%). CT, computed tomography; S/B-d NSCLC, *SMARCA4*/BRG1-deficient non-small cell lung cancer; RUL, right upper lobe; RML, right middle lobe; RLL, right lower lobe; LUL, left upper lobe; LLL, left lower lobe; SD, standard deviation.

thickened, approximately 0.5 cm thick, and was significantly enhanced in the extended scan.

FDG PET/CT FDG features

Table 4 summarizes the metabolic and staging features of FDG PET/CT scans in 12 S/B-d NSCLC patients. The SUV_{max} of the primary lung cancer lesions in 12 patients was 14.78±9.57. The FDG PET/CT revealed positive LNs in 9 (75%) patients, among whom 5 (41.67%) patients were staged as stage N3. The FDG PET/CT diagnosed distant metastases in 4 (33.33%) patients and the distant sites included: distal LNs, adrenal glands, brain, subcutaneous, bone, liver, and colorectal.

Comparison between short diameter and SUV_{max} in CT features and FDG PET/CT features

Table 5 shows the comparison between short diameter

Table 4 Summary of FDG PET/CT metabolic and staging features in 12 S/B-d NSCLC patients

Characteristic	Values
SUV_{max}	14.78±9.57
N-staging	
N (–)	3 (25.0)
N (+)	9 (75.0)
N0–2	7 (58.33)
N3	5 (41.67)
M-staging	
M0	8 (66.67)
M1	4 (33.33)

Data are presented as mean ± SD or n (%). FDG PET/CT, ^{18}F-fluorodeoxyglucose positron emission tomography-computed tomography; S/B-d NSCLC, *SMARCA4*/BRG1-deficient non-small cell lung cancer; SUV_{max}, maximum standardized uptake value; SD, standard deviation.

and SUV_{max} for CT features and FDG PET/CT features. Among the CT features of 22 patients, the short diameter of CT-diagnosed metastatic LNs was larger than that of non-metastatic LNs, and the difference was statistically significant (P=0.02). Among the FDG PET/CT features of the 12 patients, SUV_{max} was larger in the tumor group than in the lesion group and SUV_{max} was larger in the M1 group than in the M0 group, and the difference was statistically significant in both cases (P=0.001 and P=0.04, respectively).

Pathological morphology and immunophenotypic features

The patients' pathologic morphology, IHC staining, and NGS test results are summarized in *Table 6*. Totals of 7 resection samples and 16 tumor biopsy tissue samples were collected. The morphology of S/B-d NSCLC was diverse. The most common morphology resembled poorly differentiated classic non-mucinous lung adenocarcinoma. Tumor cells were cuboidal, short columnar, irregularly

Table 5 Comparison between short diameter and SUV_{max} on CT and FDG PET/CT features

Characteristic	CT scan (short diameters, cm) (N=22)	P value	PET scan (SUV_{max}) (N=12)	P value
Tumor pattern		<0.001		0.001
Lesion	1.37±0.76		6.76±4.06	
Tumor	4.15±1.47		20.97±7.57	
Degree of enhancement		0.39		
Mild to moderate enhancement	5.19±2.68		–	–
Strong enhancement	4.12±2.48		–	
Tumor site in lobe		>0.99		0.56
Central	3.34±0.56		20.20±12.02	
Peripheral	3.44±2.04		14.65±9.45	
N-staging				
N (–)	1.68±1.08	0.02	11.45±9.53	0.35
N (+)	3.79±1.73		17.31±9.50	
N0–2	3.36±1.70	0.87	13.61±8.28	0.44
N3	3.49±2.00		18.54±11.55	
M-staging				
M0	–	–	11.09±7.65	0.04
M1	–		22.58±8.26	

Data are presented as mean ± SD. SUV_{max}, maximum standardized uptake value; CT, computed tomography; FDG PET/CT, ^{18}F-fluorodeoxyglucose positron emission tomography-computed tomography; SD, standard deviation.

Table 6 Summary of pathological morphology and immunophenotypic features of 23 S/B-d NSCLC patients

Characteristic	Positive (N)	Negative (N)	Total (N)	% (positive/total)
Pathological features				
Invasion of vessels	6	1	7	85.71
Invasion of nerve	1	6	7	14.29
Invasion of pleura	1	6	7	14.29
STAS	6	1	7	85.71
Grading (poor differentiated)	10	0	10	100.00
Immunohistochemical staining results				
SMARCA4 (BRG1)	0	23	23	0
panCK	17	0	17	100.00
CK7	11	6	17	64.71
NapsinA	1	19	20	5.00
TTF-1	7	16	23	30.43
P40	0	19	19	0
P63	0	9	9	0
CD56	3	6	9	33.33
Syn	6	7	13	46.15
CgA	3	10	13	23.08
ALK-VentanaD5F3	0	9	9	0
p-TRK	0	9	9	0
Ki-67 (>50%)	8	4	12	66.67
PD-L1(22C3) (TPS ≥PS)	11	6	17	64.71
Next-generation sequencing test results				
TP53	10	–	13	76.92
KEAP1	7	–	13	53.85
STK11	4	–	13	30.77
KRAS	4	–	13	30.77
BRCA1	4	–	13	30.77
CDKN2A/2B	4	–	13	30.77
ROS1	3	–	13	23.08
FGFR1	3	–	13	23.08
BRAF	2	–	13	15.38

S/B-d NSCLC, *SMARCA4*/BRG1-deficient non-small cell lung cancer; STAS, tumor spread through airspace; TPS, tumor proportion score.

shaped, and arranged in solid nested, micropapillary, complex adenoid structures. Some tumor cells showed epithelioid or syncytial with abundant hyaline or eosinophilic cytoplasm. These cells always have a distinct nucleolus. Some areas of interstitial inflammatory cell infiltration were evident in lamellar necrosis. In addition, extracellular/intracellular mucus could be observed between the tumor cells. Intravascular tumor embolism and airspace

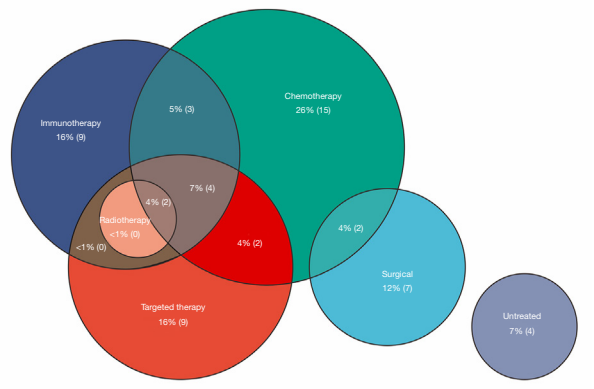

Figure 1 Summary of treatment programs of 23 S/B-d NSCLC patients. S/B-d NSCLC, *SMARCA4*/BRG1-deficient non-small cell lung cancer.

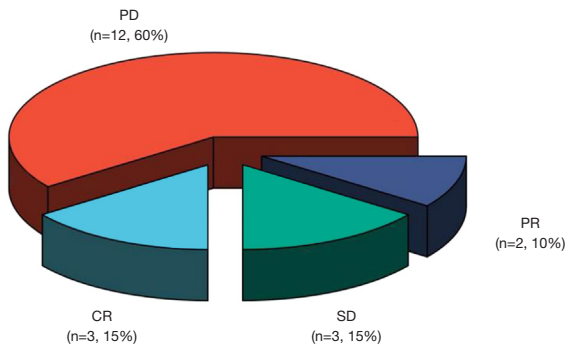

Figure 2 Summary of clinical evaluation of 20 S/B-d NSCLC patients. PD, progressive disease; PR, partial response; CR, complete response; SD, stable disease; S/B-d NSCLC, *SMARCA4*/BRG1-deficient non-small cell lung cancer.

tumor spread were commonly observed in 85.71% (6/7) of resection specimens, regardless of small tumor size.

IHC staining for BRG1 showed complete absence in all 23 patients, whereas endothelial and inflammatory cells, which served as internal positive controls, were positive. CK7 showed completely positive expression in 64.71% (11/17) of S/B-d NSCLC samples. Diffuse strong positivity for TTF-1 and NapsinA was observed in 30.43% (7/23) and 5% (1/20) of patients, respectively. Neuroendocrine markers (CD56, Syn, and CgA) showed scattered or small foci of weak expression in the lesion. In 64.71% (11/17) of cases, PD-L1 expression of ≥1%, assessed by the tumor proportion score (TPS), was detected. The Ki67 was between 20% and 90%. All patients tested were negative for p63, p40, D5F3, and p-TRK.

Among the 23 patients, the most commonly co-altered genes were *TP53* (10/13, 76.92%), *KEAP1* (7/13, 53.85%), *STK11* (4/13, 30.77%), *KRAS* (4/13, 30.77%), *BRCA1* (4/13, 30.77%), and *CDKN2A/2B* (4/13, 30.77%). *ROS1* and mutation was identified in three samples.

Treatment situation

Figure 1 summarizes the treatment options for the 23 S/B-d NSCLC patients. Four patients discontinued treatment. The treatment plan for 19 patients included is following: resection of the primary lung cancer site in 7 (36.84%) patients, chemotherapy in 15 (78.95%) patients, targeted therapy in 9 (47.37%) patients, immune checkpoint inhibitor (ICI) therapy in 9 (47.37%) patients, anti-bone metastasis therapy in 2 (10.53%) patients, and primary site irradiation in 2 (10.53%) patients. A total of 15 of these patients received combination therapy, namely: chemotherapy + targeted therapy + ICI therapy in 4 (26.67%) patients, chemotherapy + ICI therapy in 3 (20.00%) patients, primary site surgery + chemotherapy in 2 (13.33%) patients, chemotherapy + targeted therapy + ICI therapy + radiation of the primary site in 2 (13.33%) patients, and chemotherapy + targeted therapy in 2 (13.33%) patients.

Evaluation of the efficacy of treatment

Figure 2 shows the results of post-treatment clinical evaluation of 20 patients. Of these, 12 patients were classified as progressive disease (PD), 3 patients as complete response (CR), 3 patients as stable disease (SD), and 2 patients as partial response (PR).

Results of follow-up visits

Figure 3 summarizes the survival of the 23 patients. The median follow-up time for the 23 patients was 272 days (13–712 days). Among the study group, 8 patients died, 10 patients survived, and 5 patients were disconnected.

Discussion

Due to the rarity of S/B-d NSCLC, there have been more relevant studies on pathological features (1,15-17,23,24), but fewer studies on imaging, especially on FDG PET/CT features. Our current study focuses on the clinical, serum

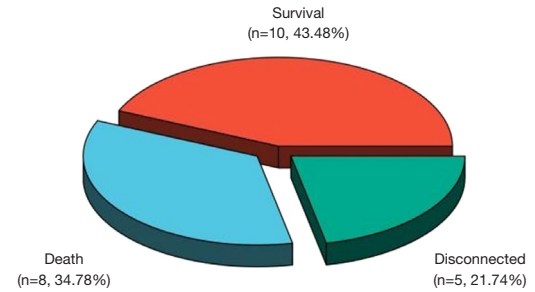

Figure 3 Summary of survival of 23 S/B-d NSCLC patients. S/B-d NSCLC, *SMARCA4*/BRG1-deficient non-small cell lung cancer.

tumor markers, imaging (including CT, MRI, FDG PET/CT), treatment regimen, and follow-up results of S/B-d NSCLC, with particular emphasis on CT and FDG PET/CT features. Our results suggest that S/B-d NSCLC occurs predominantly in male patients with a smoking history with a mean age of 62.78 years (39–77 years). More than half of the patients (56.52%) were found incidentally during physical examination. The majority of patients (82.61%) presented with moderate to advanced disease at initial diagnosis. The CT features of S/B-d NSCLC are as follows: Predominantly tumors, mostly in the peripheral lung area, with a predominantly round or roundish morphology; pleural or vascular invasion is the most common, and most of them are moderate to severe on enhanced scans. The FDG PET/CT showed FDG-avid (mean SUV_{max} of 14.78±9.57). Lung cancer-related serum tumor markers show high positivity rates for CEA, CAFRA21-1, and CA125. Pathological features are usually characterized by grading (poor differentiation), tumor spread through airspace (STAS), and invasion of vascular signs. In IHC: *SMARCA4* (BRG1), P40, P63, D5F3, and p-TRK were often found to be negative, and panCK, CK7, Ki-67 (>50%), and PD-L1 (22C3) (TPS ≥1%) were often shown to be positive. Among genetic tests, the positivity rate of *TP53* and *KEAP1* is high. Diverse treatment options, high rates of progression during treatment, and poor prognosis.

Previous studies have shown that (16,24-28) S/B-d NSCLC occurs in male patients with a smoking history and a median age ranging from 30 to 70 years. In our study, the demographic features of S/B-d NSCLC showed male prevalence, all had a history of smoking, 20 of heavy smoking, and the mean age was 62.78 years (39–77 years). Consistent with relevant reports (27), 56.52% of patients were found incidentally upon physical examination. Some patients (21.74%) also had clinical manifestations related to lung cancer (e.g., cough, sputum, hemoptysis, chest tightness) or due to metastasis (bone pain, etc.). Since one of the features of S/B-d NSCLC is highly invasive, most patients are at an intermediate to advanced stage at initial diagnosis (16,27). In our study, 82.61% of patients were in intermediate to advanced stages.

The results of our study showed that the CT features of S/B-d NSCLC were that the tumors were predominantly located in the periphery of the lung (72.73%), especially in the RUL (31.82%), LUL (36.36%). Most tumors had a predominantly round or roundish morphology, mostly subpleural, and were often associated with pleural or vascular invasion (94.46%). Most primary foci were mixed with signs of pulmonary emphysema or pulmonary bulla in the background or in the background of the entire lung (90.91%). Moderate to strong contrast enhancement was common on enhanced scans (56.53%). Several patients (86.36%) were found to have positive LNs by CT scan at the first visit, and 11 patients (50%) were found to have stage N3 disease on CT scan. Kim *et al.* (27) concluded in a small sample study (N=9) that 5 (55.6%) patients had mild centrilobular emphysema on CT scan. In our study, 90.91% of patients had signs of pulmonary emphysema or pulmonary bulla that were more extensive and even presented as total lung emphysema. We hypothesized that these signs were associated with a history of chronic or heavy smoking.

MRI is used less frequently for lung cancer. To our knowledge, we are the first to describe the MRI features of S/B-d NSCLC. We collected the MRI signs from a patient with S/B-d NSCLC. This patient's MRI signs (*Figure 4*) were as follows: a subpleural mass with inhomogeneous marked contrast enhancement seen on the contrast scan, necrotic areas in the central region, and pleural invasion. We described the MRI findings of only one patient. The value of chest MRI imaging in the diagnosis, efficacy assessment, and prognosis of S/B-d NSCLC needs to be confirmed by more relevant studies.

FDG PET/CT as a molecular imaging technique has good application value in differential diagnosis, staging, efficacy evaluation, and prognostic evaluation of lung cancer. Due to the rarity of S/B-d NSCLC, previous correlations regarding PET/CT manifestations of S/B-d NSCLC have been based on case reports (18-20). In the present study, we found that S/B-d NSCLC was predominantly characterized by FDG-avid manifestations (mean SUV_{max} 10.67±3.22, *Figures 5*-7). FDG PET/CT as whole-body imaging has advantages in staging S/B-d NSCLC. In the N stage, we

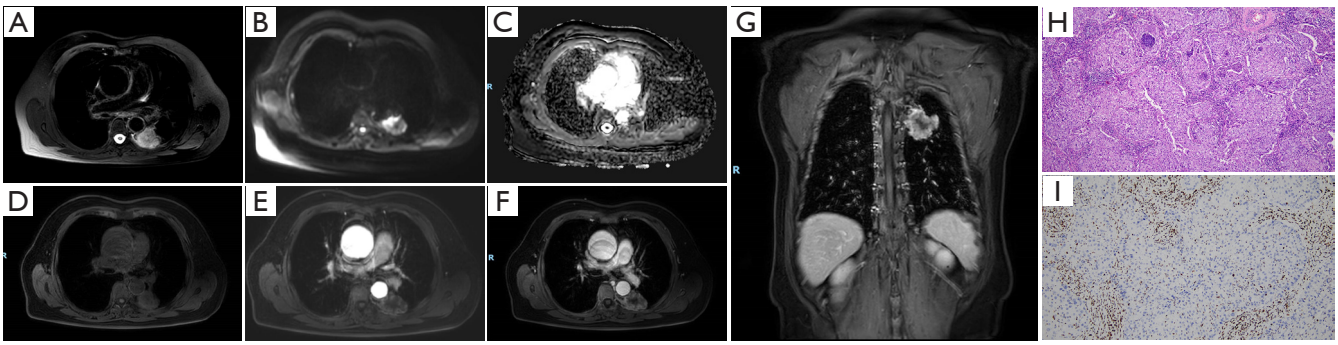

Figure 4 A 69-year-old female patient with no history of smoking. She was admitted to the hospital with the chief complaint of left-sided chest pain. Chest MRI showed a tumor in the LLL (A-E), with a size of 4.1 cm × 3.0 cm and with inhomogeneous enhancement in the enhancement scan (E-G). Serum tumor markers associated with lung cancer: CEA was 22.72 ng/mL; ProGRP was 30.93 pg/mL; CYFRA21-1 was 4.90 ng/mL; CA125 was 30.60 U/mL; NSE was 9.36 ng/mL; and SCC was 0.79 ng/mL. Puncture biopsy confirmed by pathology: S/B-NSCLC (H,I). Pathological features: poorly differentiated (H, H&E staining, 200× field of view). Immunohistochemical staining features: BRG-1 (–, I, 200× field of view). Treatment regimen: surgery + chemotherapy. Effectiveness assessment: CR. Follow-up: 155 days survival time. MRI, magnetic resonance imaging; LLL, left lower lobe; CEA, carcinoembryonic antigen; ProGRP, pro-gastrin-releasing peptide; CYFRA21-1, recombinant cytokeratin fragment antigen 21-1; CA125, carbohydrate antigen 125, NSE, neuron-specific enolase; SCC, squamous cell carcinoma antigen; S/B-NSCLC, *SMARCA4*/BRG1-deficient non-small cell lung cancer; H&E, hematoxylin and eosin; CR, complete response.

found 5 patients in the N3 stage, and FDG-avid LNs were observed bilaterally in the clavicular region, behind the peduncle of the diaphragm, in the peritoneal cavity and in the retroperitoneum, in addition to LNs in the N-stage thoracic region. In the M stage, 4 patients were classified as M1 with distant metastases including adrenal gland, brain, subcutaneous tissue, bone, liver, and colorectal. Therefore, distant metastases of S/B-d NSCLC were common and had no obvious regularity of distant metastasis as shown by FDG PET/CT features. Of particular note was the presence of subcutaneous metastases in 2 patients, with metastases in the left lumbar subcutis and the left paraspinal cord. The abovementioned subcutaneous metastases were missed during CT diagnosis. In addition, metastatic tumors, including those of the colon, are easily missed on CT scans. Therefore, FDG PET/CT as a whole-body imaging modality has a significant advantage in staging S/B-d NSCLC.

In this study, we also found that SUV_{max} was greater in the tumor group than in the lesion group, and SUV_{max} was greater in the M1 group than the M0 group (P values of 0.001 and 0.04, respectively). Therefore, in S/B-d NSCLC, we assumed that the larger the lesion at initial diagnosis, the higher the degree of malignancy. In particular, the larger the lesion and the FDG-avid, the greater the likelihood of distant metastasis. Therefore, we hypothesize that patients with suspected S/B-d NSCLC on chest CT scan, especially those with large lesions, should be recommended to undergo FDG PET/CT scanning for accurate staging and to provide a reliable imaging basis for the development of personalized clinical treatment plans.

To our knowledge, there have been no previous studies on the diagnostic value of lung cancer-related serum tumor markers in S/B-d NSCLC. In our study, we found that the positivity rates of CEA, CYFRA21-1, and CA125 were high (66.7%, 61.91%, and 57.14%, respectively), whereas the positivity rates of Pro GFR, SCC, and NSE were low (23.81%, 9.52%, and 38.10%, respectively). The value of lung cancer-related serum tumor markers for the differential diagnosis of S/B-d NSCLC and the evaluation of efficacy and prognosis needs to be confirmed by more relevant studies.

According to the literature, solid architecture, cribriform, complex gland pattern and irregular leaf or nest arrangement were the main histological structures of thoracic S/B-d NSCLC (3). The typical features of tumor cells include large epithelial cells, prominent nucleoli, and necrosis (28,29). The above features suggest that S/B-d NSCLC is a pattern of poorly differentiated or undifferentiated tumors. IHC staining is useful for distinguishing S/B-d NSCLC. The epithelial markers, including AE1/AE3, EMA, and CK7, are diffusely and/or highly expressed in *SMARCA4*/BRG1-dNSCLC (28). In

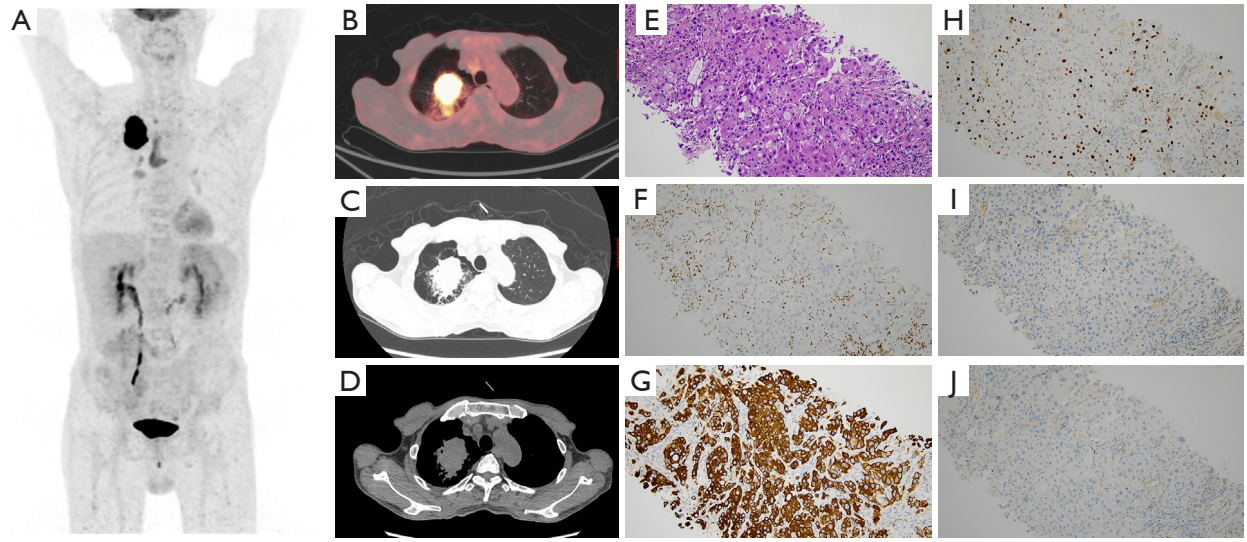

Figure 5 A 68-year-old male patient was found to have a tumor in the RUL during physical examination and had a history of heavy smoking for more than 40 years. The FDG PET/CT scan showed a tumor in the RUL (A), with a size of 4.6 cm × 3.7 cm (C), and an SUV_{max} of 25.4 (B). Chest CT enhancement showed marked enhancement. The serum tumor markers associated with lung cancer: CEA was 22.90 ng/mL; ProGRP was 34.20 pg/mL; CYFRA21-1 was 2.39 ng/mL; CA125 was 75.40 U/mL; NSE was 6.44 ng/mL; and SCC was 0.53 ng/mL. The clinical staging of the lung cancer by FDG PET/CT was cT4N2M0 (A-D). Puncture biopsy confirmed by pathology: S/B-NSCLC (E-J). Pathological features: poorly differentiated (E, H&E staining, 200× field of view). Immunohistochemical staining features: BRG-1 (–, F, 200× field of view), CK7 (3+, G, 200× field of view), KI67 (20–30%, H, 200× field of view), p40 (–, I, 200× field of view), TTF-1 (–, J, 200× field of view). The patient discontinued treatment after the diagnosis. He died after 83 days of follow-up. RUL, right upper lobe; FDG PET/CT, ^{18}F-fluorodeoxyglucose positron emission tomography-computed tomography; $SUV_{max,}$ maximum standardized uptake value; CT, computed tomography; CEA, carcinoembryonic antigen; ProGRP, pro-gastrin-releasing peptide; CYFRA21-1, recombinant cytokeratin fragment antigen 21-1; CA125, carbohydrate antigen 125; NSE, neuron-specific enolase; SCC, squamous cell carcinoma antigen; S/B-NSCLC, *SMARCA4*/BRG1-deficient non-small cell lung cancer; H&E, hematoxylin and eosin.

our study, 17 patients (100%) showed a strongly positive AE1/AE3 result, and in 6 patients, CK7 was diffusely strongly positive without IHC staining for AE1/AE3. BRG1 IHC staining is crucial for confirming the diagnosis of S/B-d NSCLC, but NGS testing for *SMARCA4* gene mutation status is not necessary if negative BRG1 protein expression is confirmed by IHC (16). In our analysis, *TP53*, *KEAP1*, *STK11*, *KRAS*, and *BRCA1* were found to be the more frequently co-mutated genes in SMARCA4/BRG1-S/B-dNSCLC. *SMARCA4* mutations were found to most commonly occur along with alterations in *TP53*, *LRP1B*, *STK11*, *KEAP1*, and *KRAS* (16). Mutations in *KEAP1* and *STK11* are associated with immunotherapy resistance in NSCLC (30). Other cohort data suggest that patients with S/B-d NSCLC may be more sensitive to immunotherapy than traditional treatments such as chemotherapy (31). In particular, it is not clear whether these patients had a genetic co-mutation in *KEAP1* and *STK11*. Therefore, carrying out a genetic test for S/B-d NSCLC appears necessary to make it easier the clinician to choose the appropriate therapy.

There is currently no standard treatment protocol for S/B-d NSCLC. In 2019, Naito *et al.* reported the first case of S/B-d NSCLC successfully treated with nivolumab (32). Wang *et al.* concluded that PD-L1 inhibitor therapy is expected to treat S/B-d NSCLC (33). A growing number of researchers are relying on ICI and ICI-based combination therapy for S/B-d NSCLC (1,13,32,34-36). In recent years, studies have concluded that a positive association between *SMARCA4* deficiency and improved responses to ICI therapy is mainly due to increased background infiltration of immune cells (35,37). It was also concluded that patients with S/B-d NSCLC have a durable response to ICI-combined chemotherapies (1,38). Further, patients with *SMARCA4* mutations have been shown to have a higher incidence of chemoresistance, early relapse, and poor prognosis compared to *SMARCA* wild-type mutations (10).

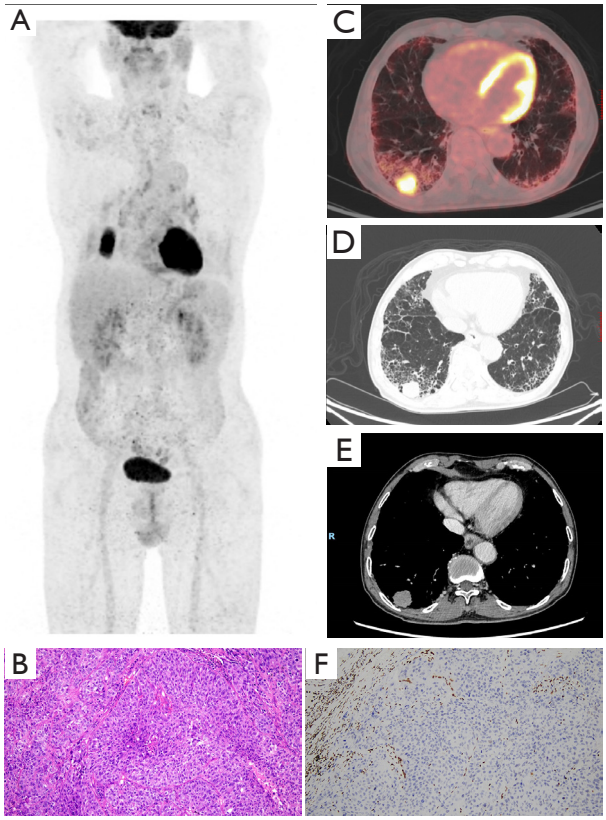

Figure 6 A 66-year-old male patient was admitted to the hospital with recurrent hemoptysis for 1 month and a history of heavy smoking for more than 40 years. The FDG PET/CT scan showed a nodule in the RLL (A,C,D,E), with a size of 2.6 cm × 2.2 cm (D), and SUV_{max} of 12.9 (C). Chest CT enhancement showed mild enhancement. The serum tumor markers associated with lung cancer: CEA was 3.98 ng/mL; ProGRP was 45.77 pg/mL; CYFRA21-1 was 4.25 ng/mL; CA125 was 20.70 U/mL; NSE was 15.89 ng/mL; and SCC was 1.74 ng/mL. Surgery confirmed that the patient had S/B-NSCLC, with postoperative staging: pT1N0M0 (B,F). Pathological features: poorly differentiated (B, H&E staining, 200× field of view). Immunohistochemical staining features: BRG-1 (–, F, 200× field of view). The patient was followed for 490 days without progression (CR). FDG PET/CT, ^{18}F-fluorodeoxyglucose positron emission tomography-computed tomography; RLL, right lower lobe; $SUV_{max,}$ standard uptake value; CT, computed tomography; CEA, carcinoembryonic antigen; ProGRP, pro-gastrin-releasing peptide; CYFRA21-1, recombinant cytokeratin fragment antigen 21-1; CA125, carbohydrate antigen 125; NSE, neuron-specific enolase; SCC, squamous cell carcinoma antigen; S/B-NSCLC, *SMARCA4*/BRG1-deficient non-small cell lung cancer; H&E, hematoxylin and eosin; CR, complete response.

Therefore, developing personalized treatment plans for patients with S/B-d NSCLC to increase utility and improve survival and quality of life is one of the remaining challenges.

We observed our participants for an average of 272 days (follow-up period 13–712 days). Our follow-up revealed that 8 patients had died (follow-up period 82–712 days), 10 patients were alive (follow-up period 155–538 days), and 5 patients were no longer available for follow-up (follow-up period 13–242 days). The 8 patients who died were in a moderate to advanced stage at the time of initial diagnosis; 3 of these patients underwent FDG PET/CT with primary focal SUV_{max} of 17.8, 25.4, and 28.9, respectively, and 1 patient had an FDG PET/CT stage of M1 at that time. Among them, 2 patients discontinued the treatment, and the remaining 6 patients chose the combination treatment program. However, efficacy assessment during treatment revealed PD in all cases. In addition, we also analyzed 10 surviving patients. Of these, 6 patients were classified as early stage and underwent surgical resection, among whom 3 patients underwent surgical resection only and all were classified as CR in later long-term follow-up. The remaining 7 patients received combination therapy, 1 of whom who had no assessment; of the remaining 6, 1 patient was classified as CR, 1 patient as PR, and 4 patients as PD. Interestingly, of the 10 patients mentioned above, 7 had undergone FDG PET/CT scans. We found that the SUV_{max} of the primary lesions ranged from 2.5 to 22.4 in these 7 patients. Among them, the SUV_{max} at the initial diagnosis of the two patients with CR was 2.5 and 6.2, respectively. Consequently, the value of FDG PET/CT scan in S/B-d NSCLC in assessing efficacy and prognosis, in addition to diagnosis and staging, is worthy of further investigation in follow-up.

The limitations of this study are as follows: First, due to the rarity of the disease studied, the sample size we collected was small and predominantly monocentric. Multi center studies are expected to be conducted in follow-up studies to increase the sample size and validate the results. Second, regarding pathology, there may be cases in the pathology database that were missed due to ack of early detection of the disease without completion of relevant immunohistochemistry (e.g., BRG1) and genetic testing. This is because in the early years, awareness of S/B-d NSCLC was limited. Third, our follow-up time was not long, and 5 patients could not be followed up for various reasons. In future research, we will further increase the

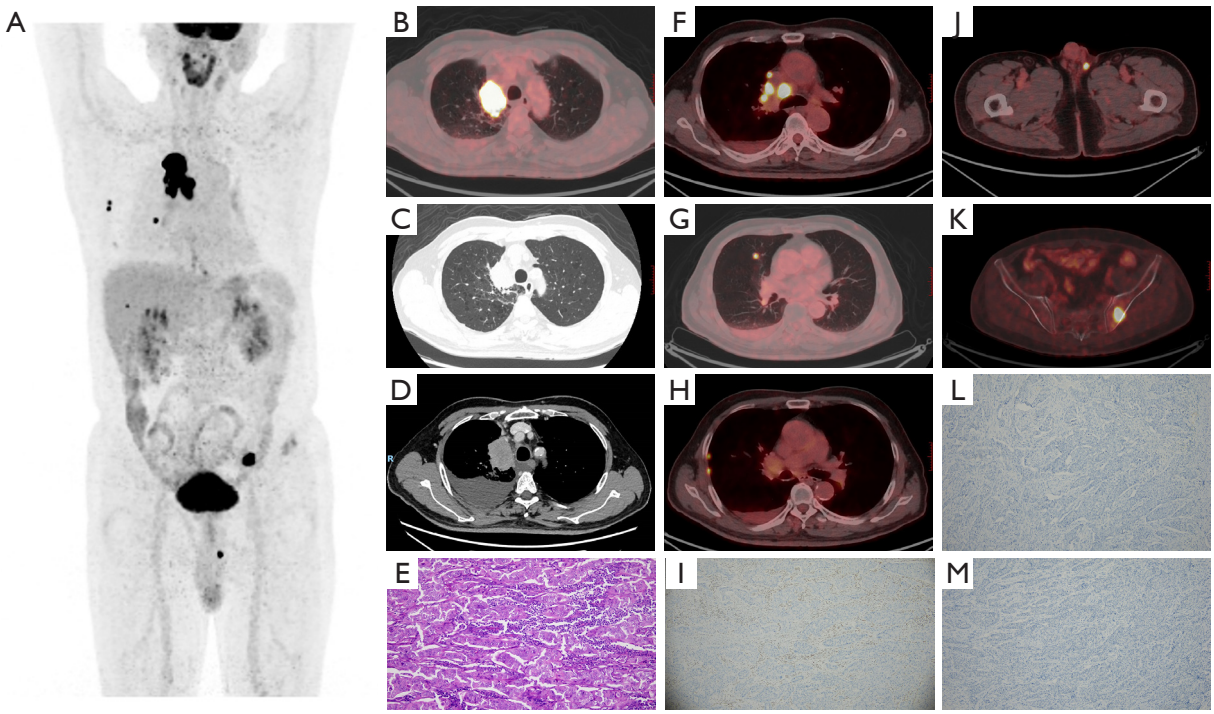

Figure 7 A 67-year-old male patient was admitted to the hospital with the chief complaint of a left inguinal tumor. With a history of heavy smoking for more than 40 years, FDG PET/CT scan revealed a tumor in the RUL (A,C,D,E), with a size of 4.1 cm × 3.2 cm and an SUV_{max} of 28.7 (C). The tumor showed moderate enhancement on chest CT. Serum tumor markers associated with lung cancer: CEA was 14.84 ng/mL; ProGRP was 40.82 pg/mL; CYFRA21-1 was 5.22 ng/mL; CA125 was 986.50 U/mL; NSE was 10.24 ng/mL; and SCC was 1.01 ng/mL. The clinical staging of the tumor by FDG PET/CT was cT4N3M1 (A-D,F,G,H,J,K). Puncture biopsy confirmed by pathology: S/B-NSCLC (E,I,L,M). Pathological features: poor differentiated (E, H&E staining, 400× field of view). Immunohistochemical staining features: BRG-1 (–, I, 200× field of view), CD56 (–, L, 200× field of view), p40 (–, M, 200× field of view). Treatment regimen: chemotherapy + targeted + ICI. Effectiveness assessment: PD. He died after 131 days of follow-up. FDG PET/CT, ^{18}F-fluorodeoxyglucose positron emission tomography-computed tomography; RUL, right upper lobe; $SUV_{max,}$ maximum standardized uptake value; CT, computed tomography; CEA, carcinoembryonic antigen; ProGRP, pro-gastrin-releasing peptide; CYFRA21-1, recombinant cytokeratin fragment antigen 21-1; CA125, carbohydrate antigen 125; NSE, neuron-specific enolase; SCC, squamous cell carcinoma antigen; S/B-NSCLC, *SMARCA4*/BRG1-deficient non-small cell lung cancer; H&E, hematoxylin and eosin; ICI, immune checkpoint inhibitor; PD, progressive disease.

sample size, open a multicenter study, strengthen the follow-up management and extend the follow-up period, and conduct relevant studies while verifying our results.

Conclusions

S/B-d NSCLC shows distinct features in epidemiology, serum tumor markers, imaging, and pathology. In particular, FDG-avid is shown in the FDG PET/CT scan. The size of the lesion and the degree of FDG avidity provide information about the degree of malignancy and the high probability of distant metastasis in S/B-d NSCLC. FDG PET/CT is recommended when S/B-d NSCLC is suspected based on CT features, especially for large lesions. The FDG PET/CT scan can help with accurate staging and individual treatment planning.

Acknowledgments

None.

Footnote

Reporting Checklist: The authors have completed the STROBE reporting checklist. Available at https://tlcr.amegroups.com/article/view/10.21037/tlcr-24-567/rc

Data Sharing Statement: Available at https://tlcr.amegroups.com/article/view/10.21037/tlcr-24-567/dss

Peer Review File: Available at https://tlcr.amegroups.com/article/view/10.21037/tlcr-24-567/prf

Funding: This study was funded by National Cancer Center/National Clinical Research Center for Cancer/Cancer Hospital & Shenzhen Hospital, Chinese Academy of Medical Sciences and Peking Union Medical College, Shenzhen (Nos. E010322003, SZ2020MS008)/Shenzhen Clinical Research Center for Cancer and Shenzhen High-level Hospital Construction Fund, and the Shenzhen Science and Technology Program of China (No. JCYJ20220818101804009).

Conflicts of Interest: All authors have completed the ICMJE uniform disclosure form (available at https://tlcr.amegroups.com/article/view/10.21037/tlcr-24-567/coif). The authors have no conflicts of interest to declare.

Ethical Statement: The authors are accountable for all aspects of the work in ensuring that questions related to the accuracy or integrity of any part of the work are appropriately investigated and resolved. The study was conducted in accordance with the Declaration of Helsinki (as revised in 2013). The study was approved by the Ethics Committee of National Cancer Center/National Clinical Research Center for Cancer/Cancer Hospital & Shenzhen Hospital, Chinese Academy of Medical Sciences and Peking Union Medical College/Shenzhen Clinical Research Center for Cancer (No. KYKT2024-19-1). All patients consented to the collection of medical information at their first visit. Inform consent is not required due to the retrospective nature of this study.

References

1. Tian Y, Xu L, Li X, et al. SMARCA4: Current status and future perspectives in non-small-cell lung cancer. Cancer Lett 2023;554:216022.
2. Wong AK, Shanahan F, Chen Y, et al. BRG1, a component of the SWI-SNF complex, is mutated in multiple human tumor cell lines. Cancer Res 2000;60:6171-7.
3. Agaimy A, Fuchs F, Moskalev EA, et al. SMARCA4-deficient pulmonary adenocarcinoma: clinicopathological, immunohistochemical, and molecular characteristics of a novel aggressive neoplasm with a consistent TTF1(neg)/CK7(pos)/HepPar-1(pos) immunophenotype. Virchows Arch 2017;471:599-609.
4. Rodriguez-Nieto S, Sanchez-Cespedes M. BRG1 and LKB1: tales of two tumor suppressor genes on chromosome 19p and lung cancer. Carcinogenesis 2009;30:547-54.
5. Wilson BG, Roberts CW. SWI/SNF nucleosome remodellers and cancer. Nat Rev Cancer 2011;11:481-92.
6. Mardinian K, Adashek JJ, Botta GP, et al. SMARCA4: Implications of an Altered Chromatin-Remodeling Gene for Cancer Development and Therapy. Mol Cancer Ther 2021;20:2341-51.
7. Imielinski M, Berger AH, Hammerman PS, et al. Mapping the hallmarks of lung adenocarcinoma with massively parallel sequencing. Cell 2012;150:1107-20.
8. Hodges HC, Stanton BZ, Cermakova K, et al. Dominant-negative SMARCA4 mutants alter the accessibility landscape of tissue-unrestricted enhancers. Nat Struct Mol Biol 2018;25:61-72.
9. Naito T, Udagawa H, Umemura S, et al. Non-small cell lung cancer with loss of expression of the SWI/SNF complex is associated with aggressive clinicopathological features, PD-L1-positive status, and high tumor mutation burden. Lung Cancer 2019;138:35-42.
10. Jones GD, Brandt WS, Shen R, et al. A Genomic-Pathologic Annotated Risk Model to Predict Recurrence in Early-Stage Lung Adenocarcinoma. JAMA Surg 2021;156:e205601.
11. Concepcion CP, Ma S, LaFave LM, et al. Smarca4 Inactivation Promotes Lineage-Specific Transformation and Early Metastatic Features in the Lung. Cancer Discov 2022;12:562-85.

12. Nambirajan A, Singh V, Bhardwaj N, et al. SMARCA4/BRG1-Deficient Non-Small Cell Lung Carcinomas: A Case Series and Review of the Literature. Arch Pathol Lab Med 2021;145:90-8.
13. Schoenfeld AJ, Bandlamudi C, Lavery JA, et al. The Genomic Landscape of SMARCA4 Alterations and Associations with Outcomes in Patients with Lung Cancer. Clin Cancer Res 2020;26:5701-8.
14. Chetty R, Serra S. SMARCA family of genes. J Clin Pathol 2020;73:257-60.
15. Dagogo-Jack I, Schrock AB, Kem M, et al. Clinicopathologic Characteristics of BRG1-Deficient NSCLC. J Thorac Oncol 2020;15:766-76.
16. Liang X, Gao X, Wang F, et al. Clinical characteristics and prognostic analysis of SMARCA4-deficient non-small cell lung cancer. Cancer Med 2023;12:14171-82.
17. Orvis T, Hepperla A, Walter V, et al. BRG1/SMARCA4 inactivation promotes non-small cell lung cancer aggressiveness by altering chromatin organization. Cancer Res 2014;74:6486-98.
18. Shen X, Yang Z, Li N. 68 Ga-DOTA-FAPI-04 PET/CT in the Detection of Thoracic SMARCA4-Deficient Undifferentiated Tumor. Clin Nucl Med 2023;48:1102-4.
19. Guo J, Liao Z, Chen Q, et al. FDG PET/CT in a Case of Thoracic SMARCA4-Deficient Undifferentiated Tumor. Clin Nucl Med 2023;48:1111-3.
20. Wumener X, Ye X, Zhang Y, et al. Dynamic and Static (18) F-FDG PET/CT Imaging in SMARCA4-Deficient Non-Small Cell Lung Cancer and Response to Therapy: A Case Report. Diagnostics (Basel) 2023;13:2048.
21. Plichta JK, Ren Y, Thomas SM, et al. Implications for Breast Cancer Restaging Based on the 8th Edition AJCC Staging Manual. Ann Surg 2020;271:169-76.
22. Detterbeck FC, Boffa DJ, Kim AW, et al. The Eighth Edition Lung Cancer Stage Classification. Chest 2017;151:193-203.
23. Long J, Chen Y, Luo X, et al. Clinical features and prognostic biomarkers in patients with SMARCA4-mutated non-small cell lung cancer. Transl Lung Cancer Res 2024;13:1938-49.
24. Longo V, Catino A, Montrone M, et al. Treatment of Thoracic SMARCA4-Deficient Undifferentiated Tumors: Where We Are and Where We Will Go. Int J Mol Sci 2024;25:3237.
25. Bell EH, Chakraborty AR, Mo X, et al. SMARCA4/BRG1 Is a Novel Prognostic Biomarker Predictive of Cisplatin-Based Chemotherapy Outcomes in Resected Non-Small Cell Lung Cancer. Clin Cancer Res 2016;22:2396-404.
26. Le Loarer F, Watson S, Pierron G, et al. SMARCA4 inactivation defines a group of undifferentiated thoracic malignancies transcriptionally related to BAF-deficient sarcomas. Nat Genet 2015;47:1200-5.
27. Kim JH, Woo JH, Lim CY, et al. SMARCA4-deficient non-small cell lung carcinoma: clinicodemographic, computed tomography, and positron emission tomography-computed tomography features. J Thorac Dis 2024;16:1753-64.
28. Zhou P, Fu Y, Tang Y, et al. Thoracic SMARCA4-deficient tumors: a clinicopathological analysis of 52 cases with SMARCA4-deficient non-small cell lung cancer and 20 cases with thoracic SMARCA4-deficient undifferentiated tumor. PeerJ 2024;12:e16923.
29. Zhou P, Fu Y, Tang Y, et al. Thoracic SMARCA4-deficient undifferentiated tumor: A clinicopathological and prognostic analysis of 35 cases and immunotherapy efficacy. Lung Cancer 2024;189:107471.
30. Kus T, Aktas G. Letter to the Editor Concerning Diminished Efficacy of Programmed Death-(Ligand) 1 Inhibition in STK11- and KEAP1-Mutant Lung Adenocarcinoma Is Affected by KRAS Mutation Status. J Thorac Oncol 2022;17:e63-4.
31. Zhang J, Zhao R, Xu H, et al. The clinicopathological features of BRG1-deficient non-small cell lung cancer and its response to immunotherapy: A single-center retrospective study. Ann Diagn Pathol 2023;67:152192.
32. Naito T, Umemura S, Nakamura H, et al. Successful treatment with nivolumab for SMARCA4-deficient non-small cell lung carcinoma with a high tumor mutation burden: A case report. Thorac Cancer 2019;10:1285-8.
33. Wang A, Jin Y, Cao Z, et al. Clinicopathological characteristics and treatment outcomes of advanced SMARCA4-deficient thoracic tumors. Cancer Med 2024;13:e6809.
34. Alessi JV, Ricciuti B, Spurr LF, et al. SMARCA4 and Other SWItch/Sucrose NonFermentable Family Genomic Alterations in NSCLC: Clinicopathologic Characteristics and Outcomes to Immune Checkpoint Inhibition. J Thorac Oncol 2021;16:1176-87.
35. Abou Alaiwi S, Nassar AH, Xie W, et al. Mammalian SWI/SNF Complex Genomic Alterations and Immune Checkpoint Blockade in Solid Tumors. Cancer Immunol Res 2020;8:1075-84.
36. Gantzer J, Davidson G, Vokshi B, et al. Immune-Desert

Tumor Microenvironment in Thoracic SMARCA4-Deficient Undifferentiated Tumors with Limited Efficacy of Immune Checkpoint Inhibitors. Oncologist 2022;27:501-11.
37. Tischkowitz M, Huang S, Banerjee S, et al. Small-Cell Carcinoma of the Ovary, Hypercalcemic Type-Genetics, New Treatment Targets, and Current Management Guidelines. Clin Cancer Res 2020;26:3908-17.
38. Kawachi H, Kunimasa K, Kukita Y, et al. Atezolizumab with bevacizumab, paclitaxel and carboplatin was effective for patients with SMARCA4-deficient thoracic sarcoma. Immunotherapy 2021;13:799-806.

Cite this article as: Wumener X, Ye X, Zhang Y, E T, Zhao J, Liang Y, Zhao J. *SMARCA4*/BRG1-deficient non-small cell lung cancer: clinical, imaging, pathological features, and follow-up results of 23 patients. Transl Lung Cancer Res 2025;14(1):107-123. doi: 10.21037/tlcr-24-567